Polymer 50 (2009) 4852–4858

Contents lists available at ScienceDirect

Polymer

journal homepage: www.elsevier.com/locate/polymer

Poly(ethylene glycol)s 2000–8000 in water may be planar: A small-angle neutron scattering (SANS) structure study

Kenneth A. Rubinson [a,b,*], Susan Krueger [a,*]

[a] NIST Center for Neutron Research, National Institute of Standards and Technology, Gaithersburg, MD 20899, USA
[b] Department of Biochemistry and Molecular Biology, Wright State University, Dayton, OH 45435, USA

ARTICLE INFO

Article history:
Received 2 June 2009
Received in revised form
12 August 2009
Accepted 15 August 2009
Available online 19 August 2009

Keywords:
Poly(ethylene glycol)
Small-angle neutron scattering
Aqueous solution structure

ABSTRACT

Poly(ethylene glycol)s of all molecular weights are highly soluble in water. Small-Angle Neutron Scattering (SANS) data has been collected on buffered ionic D_2O solutions of PEGs of nominal molecular weights 2000, 4000, and 8000 Da at a low concentration of 0.5% (w/v). The radii of gyration R_g vary as approximately $M_w^{0.5}$, which is consistent with both a Gaussian chain and a flat plate. Numerous types of experiments indicate flaws in the interpretation as a Gaussian chain. When the alternative interpretation is used, the structures in these dilute solutions are found to have a constant area stoichiometry of 1:1 water:–CH_2CH_2O– and are consistent with the data when monomeric molecules are plates of packed chains one chain thick.

1. Introduction

Among the many uses of poly(ethylene glycol)s, abbreviated PEGs, is to improve crystallizations of proteins, and the properties of these PEGs provided the motivation for this study. The PEG molecular weights (2000, 4000, and 8000 Da), and their concentrations, and solution pH and ionic concentrations in the aqueous solutions investigated here lie in the ranges common for that application. Correspondingly, the literature references cited chiefly refer to this molecular weight range.

Numerous experimental methods have been applied to aqueous PEG solutions to ascertain the properties of the water; the number of waters said to be associated per monomer unit varies from 1 to more than 10 [1–12]. However, one of the most remarkable properties is the lack of effect on water activity. Even when large fractions of the volume are filled with PEG, relatively small changes in water activity are seen [13–15]. Table 1 shows a result for PEG at 20% w/w along with other representative examples for comparison. Perhaps surprisingly, in a 67.5% w/w PEG 6000 solution—where approximately two-thirds of the water has been displaced by 6000 Da PEG—$a_w = 0.8919$ [14].

The structures and properties of poly(ethylene glycol)s (PEGs) in both the neat (pure) form and in solutions have long been subject of studies to investigate the effects of molecular weight, concentration, temperature, solvent, and ions present. A few studies by neutron methods have appeared [5,16–21].

The structures of PEG that have been found from crystallography vary greatly depending on the environment. The most well known structure is that in a pulled fiber. The molecules form 7/2 helices or twisted ribbons, which have two turns for each seven EO units [22,23]. The helix is quite open and elongated and, subsequently, without obvious interchain hydrogen bonds. The helices only form when the chains become closely packed together with the long axis in parallel and with their atomic structures lined up—which means that, e.g., corresponding oxygens of adjacent helical molecules lie in planes perpendicular to the helices' parallel long axes [24].

Among other structures that have been seen are 10/3 helices [25], a 4/1 helix [26,27], a stretched all-trans form [28] and PEG cocrystallized with $HgCl_2$ [29,30] which has a conformation approximating a sine wave, where a pair of adjacent, ethylene bridged oxygens are aligned as if a part of a crown ether and form the top of the 'wave' with the oxygen electrons pointing 'down' toward 'zero' and the next pair adjacent face the opposite direction forming the bottom of the 'wave' with the oxygen electrons projecting 'up' toward the 'zero.' A somewhat similar, planar structure is seen in a complex with $ZnCl_2$ [31].

As expected, evidence for a random-chain structure occurs in the melt [2]. Often, PEGs have been assumed to be Gaussian

* Corresponding authors. NIST Center for Neutron Research, National Institute of Standards and Technology, Gaithersburg, MD 20899, USA.
E-mail addresses: rubinson@nist.gov (K.A. Rubinson), susan.krueger@nist.gov (S. Krueger).

0032-3861/$ – see front matter © 2009 Elsevier Ltd. All rights reserved.
doi:10.1016/j.polymer.2009.08.023

Table 1
Difference in water activity in 20% w/w solutions of solutes.

Solute	Molality	$a_{w,\ pure} - a_{w,\ solution}$	Reference
PEG 6000	4.5 m[a]	0.0061	[14]
Sucrose	0.584 m	0.011	[53]
Glycerol	2.171 m	0.05	[54,55]

[a] Molality of the monomer units.

chains in water, which, however, is contradicted by descriptions such as: "highly ordered" [13];"rigid" [5] "between solid and melt forms" [32]; "pseudo stable structures" [11]; "anisotropic rods" [33].

We show below that neutron scattering data over the length scale of 15 Å–300 Å together with other chemical data suggest that PEG indeed likely possesses the form of a somewhat flexible plate one molecule thick for the molecular mass range from 2000 to 8000 Da abbreviated below as 2 k, 8 k, etc.—in salt solutions of 10 mM and 200 mM $(NH_4)_2SO_4$ as well as 3.6 M KCl and buffered to around neutral pH.

2. Experimental[1]

2.1. Preparation of samples

All PEG solutions were prepared from stock solutions to their final concentrations at least 24 h before scattering experiments. SANS shows that the equilibration for PEG 8 k from a 50% stock solution to its final concentration took longer—four days—and adjustments to sample preparation ahead of the SANS data collection were made accordingly. Over that time, the clusters present dissociated to an apparently monodisperse solution. No difference in early results were seen whether ultrapure light and heavy waters were filtered through 0.20 μm filters or not, so no filtration was used. All solutions with PEG in them were kept at ambient temperature in air and, to the greatest extent possible, in the dark. Stock solutions of PEG 2 k, 4 k, and 8 k (Fluka, purum: nominal 4 k labeled as 3500 Da–4500 Da; nominal 8 k labeled as 7000 Da–9000 Da) were 50% w/v and kept for 24 h before dilution. Stock 4 M $(NH_4)_2SO_4$ (Sigma ultra), stock 4 M KCl (GFS), stock 1 M HEPES buffer (Na salt and acid forms from Sigma), and stock 10% w/v sodium azide (Sigma) were used. All final solutions had 0.1% w/v azide as bacteriostat and 10 mM buffer.

The buffer was employed to fix the conditions as narrowly as possible. Ammonium sulfate is one of the most commonly used salts in protein crystallization buffers. The 10 mM solution was estimated as the minimum needed to level the ionic strength given the unknown and varying salt concentrations in the PEGs. The 200 mM solution is near the common working levels for crystallization. Solutions of 2.0 M $(NH_4)_2SO_4$ and greater than 3% PEG exhibited two phases after equilibration, and these multiphase solutions were not investigated by scattering. The p*D* values of the final solutions were measured to be between 6.95 and 7.25 with a glass electrode, with no correction made for isotope effects: the directly measured p*D* values were judged to be more accurate due to the simultaneous and roughly parallel changes in the buffer and electrode surface equilibria with changes in the proportions of H and D.

[1] (Disclaimer): Certain trade names and company products are identified in order to specify adequately the procedure. In no case does such identification imply recommendation or endorsement by the National Institute of Standards and Technology, nor does it imply that the products are necessarily the best for the purpose.

2.2. SANS measurements

SANS measurements were performed on the NG7 30-meter SANS instrument at the NIST Center for Neutron Research in Gaithersburg, MD [34]. The neutron wavelength, λ, was 5 Å–5.5 Å, with a wavelength spread, $\Delta\lambda/\lambda$, of 0.11. Scattered neutrons were detected with a 64 cm × 64 cm two-dimensional position sensitive detector with 128 × 128 pixels. Raw counts were normalized to a common monitor count and corrected for empty cell counts, ambient room background counts, and non-uniform detector response. Data were placed on an absolute scale by normalizing the scattered intensity to the incident beam flux. Finally, the data were radially-averaged to produce scattering intensity curves, $I(q)$, versus. q. A sample-to-detector distance of 1.3 m–1.5 m was used in order to cover the range $0.028\ \text{Å}^{-1} \le q \le 0.34\ \text{Å}^{-1}$; $q = (4\pi \sin\theta)/\lambda$ where 2θ is the scattering angle. The scattered intensities from the samples were then further corrected for buffer scattering and the varying levels of incoherent scattering from hydrogen in the samples [35]. This correction requires subtracting a contribution equal to that measured from a mixed H_2O/D_2O solution under the same conditions of neutron wavelength and geometry as the samples. When 200 mM ammonium sulfate was present, further correction for the incoherent scatter from the ammonium protons was made. This correction was not necessary for solutions with only 10 mM ammonium sulfate.

2.3. Scattering curve fitting

Fits to the scattering data were obtained using the program IGOR with macros written by Steven Kline [36]. Scattering models of regular geometric solids that were investigated included a homogeneous sphere, distribution of spheres, homogeneous prolate and oblate ellipsoids, a homogeneous cylinder, and a homogeneous cylindrical shell as well as parallelepiped, elliptical cylinder, triaxial ellipse, and Gaussian coil. In all cases where a hollow cylinder (cylindrical shell) model was used, the hole in the center decreased to zero radius within calculational error while the other parameters coincided with those found for the simple solid cylinder model. The equations for fitting the data with all these simple geometrical models as well as references to their locations in the literature can be found at ftp://ftp.ncnr.nist.gov/pub/sans/kline/Download/SANS_Model_Docs_v4.00.pdf

Some contribution to the scattering could be made by potassium binding in place of water at high potassium levels; a potassium's coherent scattering length is about equal in magnitude and opposite in sign to that of H^+. Further, the apparent radius of water of 1.4 Å approximates that of ionic K^+ of 1.52 Å. However, for it to make a contribution to the scattering, it would have to be significantly more concentrated in its association with the polymer than in the solvent since the solvent scattering has been subtracted both with low and high potassium concentrations. The possibility of binding cannot be resolved with the current data.

2.4. MALDI-TOF mass spectra

Matrix Assisted Laser Desorption Ionization (MALDI) mass spectrometry of the PEG materials were done on a Voyager DE-STR (PerSeptive Biosystems, Framingham, MA) using the reflectron mode. Desorption/ionization was produced by irradiation with pulsed UV light (337 nm) from a nitrogen laser with power set near the appearance threshold. The instrument was operated in the negative ion mode using an extraction delay time set at 200 ns and averaging 100 shots while moving over the surface. The samples were prepared as 1% w/w solutions in distilled water. These were mixed 1:1 with a matrix solution consisting of 1:1 acetonitrile:water saturated with 2-(4-hydroxyphenylazo) benzoic

acid (HABA) (Sigma) with 0.1% fluoroacetic acid added. The PEGs are composed of a number of oligomers with their fractions distributed approximately as $\sqrt{n}$. The majority of the mass lies within ±10% of the peak mass. This range of masses lies within the uncertainties of the size parameters of the models.

2.5. Calculation of the contrast

$\Delta\rho = \rho_{PEG} - \rho_{D_2O}$: ρ is the scattering length density in units of length^{-2}. The values used in calculating the contrast between the solute and the solvent, $\Delta\rho$, were found using the NCNR scattering length density calculator at www.ncnr.nist.gov/resources/sldcalc.html The values used here are: $\rho_{D_2O} = 6.33 \times 10^{-6}$ Å^{-2} for density 1.10; $\rho_{H_2O} = -0.56 \times 10^{-6}$ Å for density 1.00; $\rho_{PEG} = 0.68 \times 10^{-6}$ Å^{-2} for PEG's general formula $(C_2H_4O)_n$ for density 1.2, which is the density of the higher molecular weights of PEG. (For density 1.1, $\rho_{PEG} = 0.622 \times 10^{-6}$ Å^{-2}.) From these values, $\Delta\rho$(PEG in D_2O) $= 5.65 \times 10^{-6}$ Å^{-2}, which is the value used in all calculations. This value is required in the calculation of the molecular weight, but not for the shape analyses.

2.6. Guinier approximation calculation of R_g ($=\langle R_g^2\rangle^{1/2}$)

From neutron scattering data, the radius of gyration R_g can be calculated using Guinier's method [37], which is an approximation found to hold at low q. The data is plotted as ln ($I(q)$) versus q^2, and a straight line can be seen over some range of q that includes $R_g \cdot q \approx 1$. The slope of the straight line is

$$\mathrm{d}\ln I(q)/dq^2 = -R_g^2/3$$

from which R_g can be found. The accuracy of this calculation requires that no solute–solute motional correlation be present. However, from the measurements at higher concentrations, we know that even 0.5% PEG solutions have interfering correlations that lead to low estimated molecular weights.

2.7. Calculation of the molecular weight from I(0)

A molecular mass can be calculated that is independent of molecular structure. The equation can be found from the general formula:

$$I(0)\left[\mathrm{cm}^{-1}\right] = n(\Delta\rho)^2 V_{PEG}^2$$

where $I(0)$ is the intensity (extrapolated) of the scattering at zero angle in units of cm^{-1}, n the number density in number/cm^3, $\Delta\rho$ = the contrast in units of cm^{-2}, and V_{PEG} the volume of a single scattering center in cm^3. With the further substitutions $n = c(\mathrm{g/cm^3})\cdot N_A/M_w$ and $V_{PEG} = \bar{v}M_w/N_A$, where $\bar{v}$ is the partial specific volume in cm^3 g^{-1}, N_A Avogadro's number, and M_w the average molecular mass, we have

$$I(0) = cM_w(\Delta\rho)^2\bar{v}/N_A = \text{constant}\cdot M_w$$

With a correctly subtracted background, the absolute value of $I(0)$ provides the absolute value of the molecular mass of the scattering entity—subject to having the correct sample scattering length densities, transmissions, and correct instrumental parameters including incident flux, detector efficiency, sample area, etc. [35].

2.8. Infrared spectra

The attenuated total reflection spectra were obtained using a Bruker Equinox 55 spectrometer (Billerica, MA) with a VeeMax external reflection accessory (Pike Technologies, Madison, WI) with a ZnSe 45° total internal reflection crystal. The spectra were the average of two scans (4 cm^{-1} resolution, 2 min each) corrected for background including water vapor with Bruker's Opus software version 5.5.

3. Results and discussion

3.1. Limits on the choice of geometric model

We begin our structural inquiry by determining whether the PEG molecules (0.5% w/v PEGs in D_2O) are independent or clustered in the solution. As listed in the last column of Table 2, the molecular masses of the scattering units that are found from the extrapolated value of the scattering at zero angle, $I(0)$, indicate that the molecules, indeed are not clustered. These masses are independent of the shape [38], but do depend on an assumed molecular density.

The shape possibilities can be narrowed by plotting the dependence of the values of R_g on molecular mass. The R_gs are found from the Guinier approximation [37]. This approximation depends only weakly on the molecular structure with the error increasing with increasing anisotropy [39].

The experimental values of R_g for the 200 mM ammonium sulfate solutions shown in Table 2, column 6 are found to follow the relation $\log R_g = 0.5_6 \log M_p = 0.5_6 \log N$, where N is the degree of polymerization of the particle of mass M_p. These results are graphed in Fig. 1. This experimentally determined relationship between R_g and molecular mass can eliminate both a sphere (as $\sqrt[3]{N}$) and a long rod (as N).

This dependence of R_g on $\sqrt{N}$ is the behavior expected for two different structures: a 2-D plate or disk and a polymer formed as a Gaussian chain as found under theta conditions [40]. The Gaussian coil scatters with a result given by the Debye function for scattering,

$$D(x) = 2\left(e^{-x} + x - 1\right)\Big/x^2;\ x = (qR_g)^2$$

and the best-fitting R_g values for the Gaussian coil fits are shown in column 7 of Table 2.

A plate-like structure can be fit by many model geometrical shapes. Such models include triaxial ellipsoides, elliptical orthogonal cylinders, and parallelepipeds (orthorhombic prisms). We choose to use the last of these three while noting that the best

Table 2
SANS data-fitting parameters for 0.5 wt% PEG solutions in D_2O as an orthogonal parallelepiped and a Gaussian chain with $\Delta\rho = 5.65$ e-6.

PEG MW $[(NH_4)_2SO_4]$	Side A (Å)	Side B (Å)	Side C (Å)	R_g for fitted prism (Å)[a]	R_g from Guinier plot[b]	R_g for fitted Gaussian (Å)	$I(0)$ (cm^{-1})/ MW calculated (kDa)[c]
PEG 2 k 10 mM	4	16	57	$17._2$	$14._9$	$16._4$	0.035/1.8 kDa
PEG 2 k 200 mM	5	23	48	$15._4$	$12._1$	$16._2$	0.055/2.9 kDa
PEG 4 k 10 mM	3	28	79	$24._2$	$24._2$	$24._8$	0.055/2.9 kDa
PEG 4 k 200 mM	4	27	78	$24._0$	$19._0$	$24._1$	0.060/3.2 kDa
PEG 8 k 10 mM	3	42	102	$31._9$	$25._7$	$36._2$	0.104/5.5 kDa
PEG 8 k 200 mM	3	43	97	$30._5$	$26._3$	$36._5$	0.100/5.3 kDa

[a] For a prism of edge lengths A, B, C: $R_g^2 = [(A^2 + B^2 + C^2)/12]$.
[b] Calculated by the approximation of Guinier [37].
[c] Calculated by the method of Jacrot and Zaccai [56]. Assumes the density of molecular PEG is 1.2 g cm^{-3}.

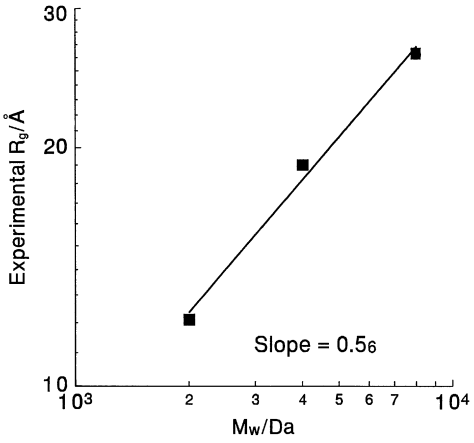

Fig. 1. Log–log plot of R_g versus PEG molecular weight. The uncertainty in the slope is difficult to evaluate, but the slope clearly differs from $M_w^{1/3}$ or M_w^1.

fitting volumes and R_g values of all three types are similar, but the parallelepiped benefits from having orthogonal variables. The quality of a fit by parallelepipeds with homogeneous scattering length densities can be seen in Fig. 2. The size variables of the plate are shown in columns 2, 3, and 4 of Table 2, while the R_g calculated from them are in column 5.

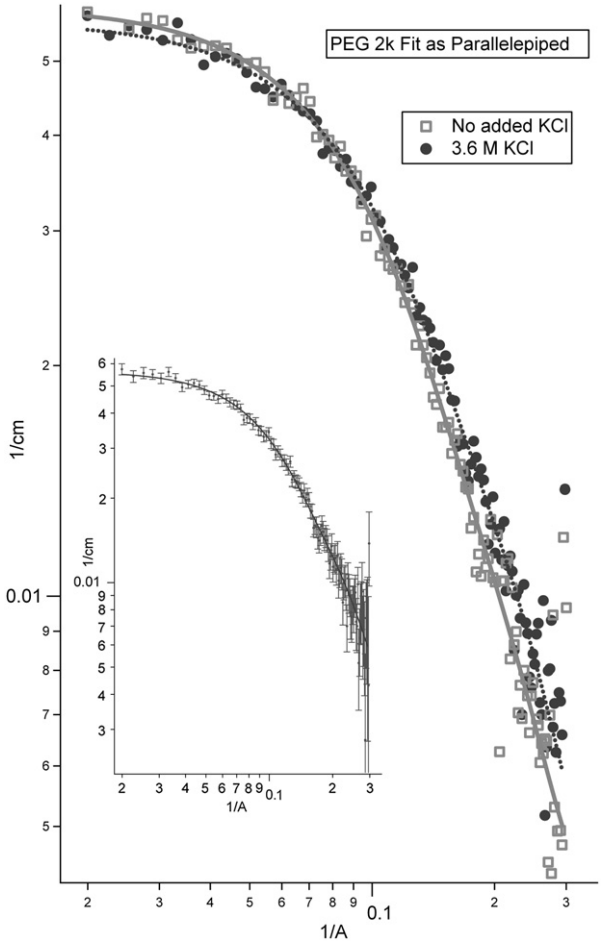

Fig. 2. Data of PEG 2000 with minimal KCl and 3.6 M KCl buffers. The best fit lines are for model parallelepipeds as annotated in Table 3. The inset shows one data set with associated error bars.

Numerous other types of models were tried. Among these are flexible polymers modeled with variables of contour length, Kuhn length, and cross section. Such models are severely constrained by the mass distributions known from MALDI and the subsequent limits of contour lengths, as well as the limitations of organic molecule structural regularities. Such modeling did not simultaneously fit the data well while conforming to the limitations imposed by the mass distribution and descriptive chemistry.

Comparable solutions of PEG 2000 in a minimum of KCl and in 3.6 M KCl also were run to test the possibility mentioned by Rodrigues et al. [41] that the high KCl reduces the chain mobility in PEG 2000. High K^+ or high Cl^- also might disrupt the structures of the plate or cause the structural collapse of a more diffuse form. The K^+ might bind in the manner of a crown ether or the Cl^- as a member of the Hofmeister series. The results of this comparison are shown in Fig. 2, and the fits are listed in Table 3. The values of the experimental R_gs indicate that the dimensions of the scattering structures are only slightly reduced in the high KCl solution compared to the low ionic strength solution.

In addition to the PEGs' small sizes, these small molecules are relatively poor scatterers in H_2O solution because their scattering strength is nearly the same as the light water's. As a result, the majority of the scattering, with the results reported here, was carried out on D_2O solutions. However, no significant difference in the molecular parameters derived from the scattering was seen with D_2O:H_2O 75:25 by volume as solvent, and we believe that the results for the D_2O solutions hold for H_2O as well.

3.2. Choosing between a plate and a Gaussian chain

The general assumption about PEGs in water is that they form Gaussian or expanded Gaussian coils, and the interpretations of experimental data depend on that assumption, e.g., see Branca [20] or Breen [42]. However, a number of measurements described in this section contradict this expectation, which leads us to examine the structure as possibly being a plate.

In the data collected here and shown in Tables 2 and 3, the agreement of the Guinier equation values of R_g agree, overall, better with the values of the parallelepipeds than with the Gaussian coils'. The discrepancies that remain in the parallelepiped values may originate in the large anisotropy of the structures [39].

Another exception is found for the diffusion coefficient, which is expected to change with approximately $M_w^{-0.5}$, and some experimental exponents around that value have been found. Nevertheless, when diffusion coefficients for PEGs fractionated with supercritical fluid chromatography were measured by NMR over the homologous series from ethylene glycol to PEG 1600, the diffusion coefficient showed a dependence on $M^{-0.43}$ [43] The magnitude suggests a compressed structure rather than a random coil, but most of the range should be classified as oligomers rather than polymers. Nevertheless, the entire range lies along the same straight log–log line.

Table 3
SANS data-fitting parameters for 1 wt% PEG 2000 solutions in D_2O as an orthogonal parallelepiped and Gaussian chain with $\Delta\rho = 5.65$ e-6.

Sample	Side A (Å)	Side B (Å)	Side C (Å)	R_g for fitted prism (Å)[a]	R_g from Guinier plot[b]	R_g for fitted Gaussian (Å)
PEG 2 k 0 added KCl	2	22	45	$14._6$	$13._7$	$15._4$
PEG 2 k 3.6 M KCl	2	16	44	$13._6$	$13._0$	$14._8$

[a] For a prism of edge lengths A, B, C: $R_g^2 = [(A^2 + B^2 + C^2)/12]$.
[b] Calculated by the approximation of Guinier [37].

Despite that apparently simple log–log functionality, precise measurements of the PEGs' apparent specific volumes at infinite dilution obtained by Kirinčič and Klofutar [9] show different behavior, as can be seen in the log–log graph of Fig. 3. Apparently the solvation behavior of PEGs below approximately 1 kDa differs from that for PEGs in the range 1–35 kDa. Their overall structures apparently differ in the two ranges.

With a fixed molecular weight, a change in structure also apparently occurs as seen in a break in the concentration dependent changes in the bulk compressibility of aqueous PEGs 2 k, 4 k, and 8 k [44]. The compressibility changes with concentration below about 7% w/v PEG differs from those above that level. The PEGs appear to be controlling about three layers of water. (In this characteristic, the PEGs seem to mirror collagen [45].) At the concentration where the outer waters must be shared, there appears to be a change in the overall structure of PEG + water. The same break is seen in infrared spectra (unpublished data). Such a sharp break would be unexpected from flexible coils that would gradually begin to interact at their peripheries as their concentrations increase.

PEG is nearly universally described as hydrophilic because of its high solubility in water, but Özdemir and Güner [46] find that among THF, Chloroform, DMSO, methanol, and water, water is the weakest solvent for PEG. If that is the case, then the PEG would be expected to be found in a structurally compressed form, not a Gaussian coil or extended form. This point of view is supported by the values of the experimental R_gs in low ionic strength compared to high KCl solution as shown in Table 3. The dimensions of the scattering structures remain essentially the same and there is no indication of a collapse or expansion of a putative expanded Gaussian coil.

Other evidence points to the hydrophobic nature of PEG controlling its aqueous environment. For example Huot [47] finds that even ethylene glycol is predominantly hydrophobic. Nishi et al. [48] have shown that even ethanol forms clusters in water beginning with some dimers appearing by 28 mM (0.0005 mole fraction) ethanol at 35°. And, finally, Tager et al. [49] suggests that polymers with lower critical solution temperatures—such as PEG—have hydrophobic hydration predominating.

We note that our data was taken well below the theta temperature under the ionic conditions used. For example, Özdemir and Güner [50] estimate the theta temperature in pure water to be (51 ± 4)°C and to change only a few degrees over the molecular weight range used here. Others obtain much higher values as noted in the Özdemir paper. Among the others are Boucher and Hines [51], and since the molecular weight dependence is so small, we can use their estimates of a theta temperature in pure water of (96 ± 3) °C for PEG 20 k and also their values under our salt conditions: for 200 mM K_2SO_4 65 °C and for 3.2 M KCl 35 °C. Our experiments were run at 22 °C. Only the one experiment that in 3.6 M KCl was closer than 30 °C below any estimated theta temperature regardless of the method employed to find it.

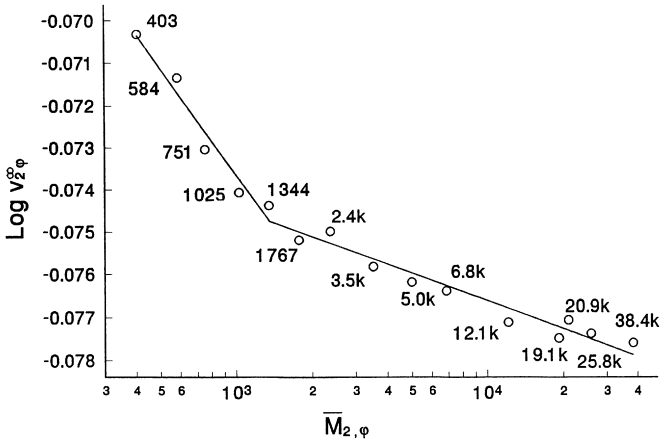

Fig. 3. A plot of the logarithm of the apparent specific volume of the PEGs at infinite dilution at 291.15°, $v_{2\varphi}^{\infty}$ in $cm^{-3}\,g^{-1}$, versus the measured viscosity average molecular mass, on a logarithmic scale. The data is from Kirinčič and Klofutar [9].

Finally, we note that the parallelepiped structures with the dimensions listed in Table 2 are consistent with the radius ratio determined long ago by viscometry [33].

3.3. Stoichiometry and the plate structure

The purpose of this section is to investigate whether water is part of the plate-like structure of these PEG molecules. It is necessary to use the surface area of the largest face of the parallelepiped for a number of reasons both from experimental limitations and from the chemistry of the surface. First, experimentally, there is significant scatter of the thickness values listed in Table 2. This scatter is not surprising since the estimated dimension results from extrapolation well beyond the high-q limit of the experimental data, a limit equivalent to a length about 15 Å. The quantitative consistency among the paired conditions appears to improve with increasing molecular mass, and this is as expected. The reason for the improvement is that the long dimension of PEG 2 k lies close to the high-q limit, which leaves little of the scattering curve to fit and extrapolate. In comparison, for the PEG 8 k, the fitted portion of the curve is longer, and the extrapolation is relatively shorter.

The fitted thickness of the polymer structure in the range 2–5 Å suggests that the molecular structure is about one chain thick. However, the accuracy of the shortest lengths also depends on a number of specific possible ambiguities that the solution chemistry at the interface imposes on the scattering results. First, note that the smallest modeled values of the thickness are less than the 4.02 Å diameter of methane. This is reasonable since the neutrons scatter from the nuclei, and the distance between a methylene's two hydrogen nuclei is only 1.8 Å. In addition, although the scattering of the solvent D_2O is subtracted, any overall orienting of the solvent with the water's deuteriums toward or away from the interface which has the effect of partitioning the deuteriums' distance relative to the surface means that the effective bulk-matching surface would be displaced. In other words, the nature of the changeover between the contrasting molecules and the solvent is less certain because the interface is such a large fraction of the single-molecule thickness. This chemical mechanism provides yet more uncertainty to the short dimension.

Because of the short dimension's uncertainty, we use only the area of the largest surface of the best fitting parallelepiped to investigate structural regularities. Also, the lengths of both sides of these surfaces lie within the instrument's range.

The areas of these plate surfaces can be compared with the molecular areas of the corresponding PEGs projected onto the surface. The PEG areas are computed as the product of the contour length and diameter. The contour length is calculated as the product of the number of bonds times the 1.4 Å bond length and the diameter is taken as the 4.02 Å diameter of methane. For example PEG 2000 has approximately 45 EO monomers, and the chain is, then, about 135 atoms long, which gives a contour length of $135 \times 1.4 = 189$ Å. The area projection results by multiplying the length by its 4.02 Å diameter: $189 \times 4.02 = 760$ $Å^2$. As shown in the fifth column of Table 4, the areas of the largest surfaces, B × C, are larger than the total areas of the molecules by a quite regular factor of about 1.4 for the three molecular weights.

This apparent expansion of the areas of the plates compared to the area of the molecule indicates that water is likely contained in

Table 4
Areas and the stoichiometry of PEGs.

M_w PEG/Da	Number EO	EO area[a]/Å	Area $B \times C$/Å	Meas/EO area	Meas-EO = water area	No. waters[b]
2000	45	760	$16 \times 57 = 912$	1.2	152	22
			$23 \times 48 = 1104$	1.45	344	50
4000	90	1520	$28 \times 79 = 2212$	1.45	692	101
			$27 \times 78 = 2106$	1.38	586	86
8000	180	3040	$42 \times 102 = 4284$	1.38	1244	183
			$43 \times 97 = 4171$	1.37	1131	166

[a] The calculated cross sectional area equals the contour length (number of bonds × 1.4 Å) × 4.02 Å diameter.
[b] The number of waters = total water area/single water area. The latter area is that of closely packed waters: a hexagon superscribed around the 1.4 Å radius circle of a water molecule. Hexagon area = 3.46 r^2 = 6.8 Å^2.

the plane and expands the structure of chains. However, this structure is tightly packed since the compressibility of the PEGs decreases by an order of magnitude in the aqueous solution compared the neat polymer [44].

We can derive the two-dimensional stoichiometry by dividing the areas that are not PEG (Column 6, Table 4) by the area occupied by a water molecule if it were closely packed in two dimensions; this is the area of a hexagon superscribed about a circle with the commonly accepted water radius of 1.4 Å. This area is 6.8 Å^2. The number of waters associated with each molecular weight found in this way is given in the rightmost column of Table 4. We see a common stoichiometry of one water per EO unit. This consistency of stoichiometry provides another reason to accept the flat plate as being the correct choice of structure.

Note that the 1:1 EO:water stoichiometry is that of a two-dimensional projection. We cannot discern any difference if two stacked waters occupy the area or only a single water resides in the space.

Our resolution does not inform us of the various possible PEG structures within the plate, and any of the structures mentioned in the Introduction are possibly present. For example, the thickness of the plate fits in the range of the diameter of the PEG 7/2 helices found in a pulled-fiber crystalline solid [23], which might then be a possible motif. However, a characteristic of that helical form is a narrow infrared band at 1118 cm^{-1} [24]. Total-internal-reflection infrared spectra of these PEG solutions in the concentration range 1%–20% w/v showed no such band. The presence of this band is known to require an extended lattice of triangularly packed PEGs [52]. However, it is not established whether an extended plane of parallel helices each with only two opposing neighbors would have the 1118 cm^{-1} band. So from that criterion, the possibility of the plate having a substructure of 7/2 helices cannot be completely rejected. On the other hand, Maxfield and Shepard [2] investigated relatively concentrated aqueous solutions of PEG (>30%) and found that the helical structure of the crystalline material is already lost with that smaller amount of water added to the solid.

A number of other structures observed by x-ray crystal analysis also could form plates of parallel chains [28]. The planar zigzag structure has the PEGs in the crystal with the chains separated by about 4½ Å in both directions normal to the long axis. In one direction, the oxygens lie aligned together in the plane. In the other, the oxygens lie in lines alternating above and below the plane. Another possible structure would form a thicker plane: this PEG structure is found when the chain weaves among cocrystallized $HgCl_2$ where the PEG's oxygens bind the mercury ions with half a crown [28,29]. Finally, another possibility is the flat structure woven around the zinc ions in the $ZnCl_2$–PEG complex [31].

Finally, as noted earlier, just as the density change shown in Fig. 3 indicates different structural motifs, infrared spectra of the aqueous solutions indicate the same break point. Infrared bands found for concentrations of PEG 2 k to PEG 8 k at less than 5% w/v are also seen for PEG 1 k, but not for lower molecular masses. In other words, these plate-like structures do not form below PEG 1000, that is, when the two "ends" have less than about 10 monomer units. In agreement with this dichotomy, Breen et al. [42] discerned from the variations of NMR decay times, that the first three monomer units at the ends of the chains have less restricted mobility. These findings suggest that the outside edges of the plates are likely quite flexible, and may account for much of the variation of dimensions seen in the PEG 2 k, where the edges are a significant fraction of the whole. The PEG 4 k and 8 k appear more reproducible experimentally because the flexible ends comprise a much smaller fraction. Nevertheless, the flexibility of the ends and the fact that the structure does not appear until the molecular mass exceeds 1000 Da suggest that the overall structure will be flexible to some degree.

4. Conclusions

Small-angle neutron scattering (SANS) data has been collected on buffered ionic D_2O solutions of PEGs of nominal molecular weights 2000, 4000, and 8000 Da at a low concentration of 0.5% (w/v). Two different possible structures are consistent with the square root dependence of R_g on the molecular weight: a Gaussian coil and a flat plate. Various measurements are anomalous with a coil structure and point to a tight structure. The neutron scattering data is consistent with monomeric molecules in the shape of flat plates of packed chains one chain thick that contain water with the same stoichiometric amount for all three molecular weights: one water per ethylene oxide unit. Infrared spectral data suggest such structures are not formed in PEGs with molecular weights below 1000 Da. However, since we have not investigated PEGs with molecular weights higher than 8000 Da, we cannot surmise what structures might be present for those.

Acknowledgments

The authors wish to thank Curt Meuse for running infrared spectra and Joseph Hubbard for illuminating discussions.

References

[1] Couper A, Stepto RFT. Trans Faraday Soc 1969;65:2486–96.
[2] Maxfield J, Shepherd IW. Polymer 1975;16:505–9.
[3] Antonsen KP, Hoffman AS. In: Harris JM, editor. Poly(ethylene glycol) chemistry: biotechnical and biomedical applications. New York: Plenum; 1992.
[4] Zhlyakova TA, Nikolov OT, Maleev BY. Zhurnal Fizicheskoi Chimii 1993;67(7):1396–400.
[5] Bieze TWN, Barnes AC, Huige CJM, Enderby JE, Leyte JC. J Phys Chem 1994a;98:6568–76.
[6] Jannelli MP, Magazu S, Maisano G, Majolino D, Migliardo P. J Mol Struct 1994;322:337–43.
[7] Crupi V, Jannelli MP, Magazu' S, Maisano G, Majolino D, Migliardo P, et al. J Mol Struct 1996;381:207–12.
[8] Tirosh O, Barenholz Y, Katzhendler J, Priev A. Biophys J 1998;74:1371–9.
[9] Kirinčič S, Klofutar C. Fluid Phase Equilib 1998;155:311–25.
[10] Branca C, Magazu S, Migliardo F, Romeo G. J Mol Liq 2003;103–104:181–5.
[11] Schmelzer CEH. J Mol Struct 2004;699:47–51.
[12] Zwirbla W, Sikorska A, Linde BBJ. J Mol Struct 2005;743:49–52.
[13] Lakhanpal ML, Chhina KS, Sharma SC. Indian J Chem 1968;6:505–9.
[14] Grossmann C, Tintinger R, Zhu J, Maurer G. Fluid Phase Equilibria 1995;106:111–38.
[15] Ninni L, Camargo MS, Meirlles AJA. Thermochim Acta 1999;328:169–76.
[16] Dahlborg U, Dimic V. Phys Scr 1988;37:93–101.
[17] Barnes AC, Bieze TWN, Enderby JE, Leyte JC. J Phys Chem 1994d;98:11527–32.
[18] Thiyagarajan P, Chaiko DJ, Hjelm RPJ. Macromolecules 1995;28:7730–6.
[19] Hakem IF, Lal J, Bockstaller MR. Macromolecules 2004;37:8431–40.
[20] Branca C, Faraone A, Magazù S, Maisano G, Migliardo P, Triolo A, et al. J Appl Crystallogr 2000;33:709–13.
[21] Alessi ML, Norman AI, Knowlton SE, Ho DL, GS C. Macromolecules 2005;38:9333–40.

[22] Tadokoro H, Chatani Y, Yoshihara T, Tahara S, Murahashi S. Makromol Chem 1964;73:109–27.
[23] Takahashi Y, Tadokoro H. Macromolecules 1973;6(5):672–5.
[24] Vanderah DJ, Arsenault J, La H, Gates RS, Silin V, Meuse CW. Langmuir 2003;19:3752–6.
[25] Point JJ, Coutelier C, Villers D. J Phys Chem 1986;90:3277–82.
[26] Tadokoro H. Macromol Rev 1966;1:119–72.
[27] Chenite A, Brisse F. Macromolecules 1991;24:2221–5.
[28] Takahashi Y, Sumita I, Tadokoro H. J Polym Sci Phys Edn 1973;11:2113–22.
[29] Iwamoto R, Saito Y, Hideaki I, Tadokoro H. J Polym Sci A-2 1968;6:1509–25.
[30] Yokoyama M, Ishihara H, Iwamoto R, Tadokoro H. Macromolecules 1969;2:184–92.
[31] Staunton E, Christie AM, Martin-Litas I, Andreev YG, Slawin AMZ, Bruce PG. Angew Chem Int Ed 2004;43:2103–5.
[32] Branca C, Magazu S, Maisano G, Migliardo P, Villari V. J Phys Condens Mater 1998;10:10141–57.
[33] Thomas DK, Charlesby A. J Polym Sci 1960;42:195–202.
[34] Glinka CJ, Barker JG, Hammouda B, Krueger S, Moyer JJ, Orts WJ. J Appl Crystallogr 1998;31(3):430–45.
[35] Rubinson KA, Stanley C, Krueger S. J Appl Crystallogr 2008;41:456–65.
[36] Kline SR. J Appl Crystallogr 2006;39:895–900.
[37] Guinier A. Ann Phys 1939;12:161–237.
[38] Porod G. In: Glatter O, Kratky O, editors. Small angle X-ray scattering. London: Academic Press; 1982 [chapter 2].
[39] Glatter O, Kratky O. Section 2.III.B. London: Academic Press; 1982.
[40] Doi M. Introduction to polymer physics. Oxford: Clarendon Press; 1996.
[41] Rodrigues CG, Machado DC, Chevtchenko SF, Krasilnikov OV. Biophys J 2008; 95:5186–92.
[42] Breen J, van Duijn D, de Bleijser J, Leyte JC. Ber Bunsenges Phys Chem 1986;90:1112–22.
[43] Shimada K, Kato H, Saito T, Matsuyama S, Kinugasa S. J Chem Phys 2005;122:244914.
[44] Rubinson KA, Hubbard J. Polymer 2009;50:2618–23.
[45] Leikin S, Parsegian VA, Yang W-H, Walrafen GE. Proc Natl Acad Sci USA 1997;94:11312–7.
[46] Özdemir C, Güner A. Eur Polym J 2007;43:3068–93.
[47] Huot J-Y, Battistel E, Lumry R, Villeneuve G, Lavallee J-F, Anusiem A, et al. J Soln Chem 1988;17(7):601–36.
[48] Nishi N, Takahashi S, Matsumoto M, Tanaka A, Muraya K, Takamuku T, et al. J Phys Chem 1995a;99:462–8.
[49] Tager AA, Safronov AP, Berezyuk EA, Galaev IY. Colloid Polym Sci 1994;272: 1234–9.
[50] Özdemir K, Güner A. J Appl Polym Sci 2006;101:203–16.
[51] Boucher EA, Hines PM. J Polym Sci Polym Phys Ed 1976;14:2241–51.
[52] Kobayashi M, Sakashita M. J Chem Phys 1992;96(1):748–60.
[53] Robinson RA, Stokes RH. Electrolyte solutions. 2nd ed. London: Butterworths; 1959. p. 478.
[54] Braun JV, Braun JD. Corrosion 1958;14:17–8.
[55] Newman AA. Glycerol. Cleveland: CRC Press; 1968. Table 1.
[56] Jacrot B, Zaccai G. Biopolymers 1981;20:2413–26.